ChemPhysChem

Concept
doi.org/10.1002/cphc.202200384

Chemistry Europe
European Chemical Societies Publishing

www.chemphyschem.org

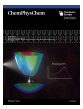

Photoinduced Intervalence Charge Transfers: Spectroscopic Tools to Study Fundamental Phenomena and Applications

Ivana Ramírez-Wierzbicki,[a, b] Agustina Cotic,[a, b] and Alejandro Cadranel*[a, b, c]

Dedicated to Prof. Silvia Braslavsky on the occasion of her 80th birthday.

The exploitation of excited state chemistry for solar energy conversion or photocatalysis has been continuously increasing, and the needs of a transition to a sustainable human development indicate this trend will continue. In this scenario, the study of mixed valence systems *in the excited state* offers a unique opportunity to explore excited state electron transfer reactivity, and, in a broader sense, excited state chemistry. This Concept article analyzes recent contributions in the field of photo-induced mixed valence systems, *i.e.* those where the mixed valence core is absent in the ground state but created upon light absorption. The focus is on the utilization of photoinduced intervalence charge transfer bands, detected via transient absorption spectroscopy, as key tools to study fundamental phenomena like donor/acceptor inversion, hole delocalization, coexistence of excited states and excited state nature, together with applications in molecular electronics.

Introduction

Mixed valence (MV) systems are those including the same (or very similar) redox active fragment(s) in different formal oxidation states, creating the simplest donor-acceptor moieties, {D–A}.[1] MV systems were used to explore a wide variety of chemical scenarios for electron transfer,[2–8] from transition metals[9] to organics[10] and other main-group elements,[11] from solution to rigid media[12] or the solid state.[13] MV systems have been traditionally studied in the ground state, using electrochemical techniques,[14] spectroscopic methods,[15,16] or combinations of both. However, in a context of intensive use of excited state chemistry for solar energy conversion or photocatalysis, the study of MV systems *in the excited state* is required, since they offer a unique opportunity to explore excited state electron transfer reactivity in particular, and excited state chemistry in general.

Ground state MV systems are usually prepared from a non-MV precursor {D–D'} or {A'-A} via (electro)chemical oxidation or reduction of D' or A' fragments, respectively, generating a {D–A} MV system (Figure 1). Observation of D→A intervalence charge transfers (IVCT) using vis-NIR absorption spectroscopy allows for the determination of key parameters related to the thermal D→A process like the donor-acceptor electronic coupling H_{DA}. Photoinduced MV (PIMV) systems are also prepared from non-MV starting materials, but use light to trigger charge transfer events that oxidize or reduce D' or A' fragments. Transient {D–A(C)} MV cores are generated, where C is the counterpart also generated in the charge transfer event (Figure 1). The influence of C in the PIMV properties of {D–A(C)} systems is determinant, which makes them inherently different from ground state analogs. Key to address PIMV systems is ultrafast transient absorption spectroscopy (TAS), which allows the detection of photoinduced IVCT (PIIVCT) absorptions in the NIR and the determination of excited state electronic couplings.

Until recently, and despite more than 60 years of investigations about ground state MV systems, very few PIMV systems had been reported and studied as such. Earliest examples from the 80s study photoinduced electron transfer and explicitly refer to the creation of PIMV cores using light, where no MV system was present in the ground state.[17,18] Since then, PIMV systems have been studied indirectly, analyzing absorption and emission bandshapes,[19,20] resonant Raman and electrooptical absorption spectroscopies[21–23] on non-MV systems, or directly, using time resolved IR spectroscopy[24] or UV-vis TAS.[25,26] However, to the best of our knowledge, the first observations of PIIVCT bands date from the 90s,[27–29] with only a handful of later reports.[30–33] In this Concept article, the focus is on the opportunities to study fundamental electron transfer phenomena and applications, that arise from the observation of PIIVCT bands using TAS and modelling of the results thereof.

[a] I. Ramírez-Wierzbicki, A. Cotic, Dr. A. Cadranel
Instituto de Química Física de Materiales, Medio Ambiente y Energía (INQUIMAE), CONICET – Universidad de Buenos Aires
Pabellón 2, Ciudad Universitaria, C1428EHA, Buenos Aires, Argentina
[b] I. Ramírez-Wierzbicki, A. Cotic, Dr. A. Cadranel
Departamento de Química Inorgánica, Analítica y Química Física, Universidad de Buenos Aires, Facultad de Ciencias Exactas y Naturales
Pabellón 2, Ciudad Universitaria, C1428EHA, Buenos Aires, Argentina
E-mail: acadranel@qi.fcen.uba.ar
[c] Dr. A. Cadranel
Department Chemie und Pharmazie, Physikalische Chemie, Friedrich-Alexander-Universität Erlangen-Nürnberg
Egerlandstraße 3, 91058 Erlangen, Germany
E-mail: ale.cadranel@fau.de

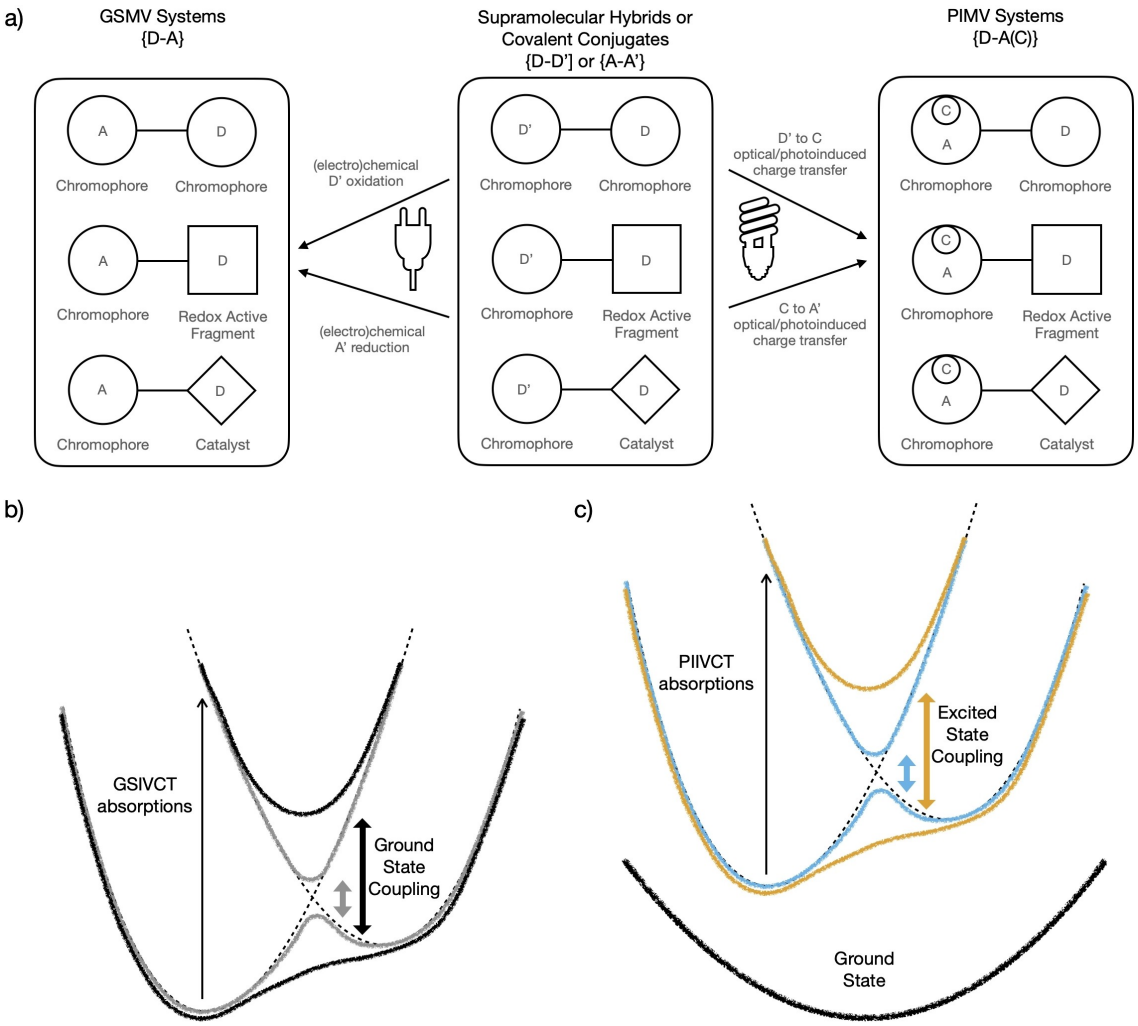

Figure 1. a) General molecular designs related to ground-state mixed valence (GSMV) and photoinduced mixed valence (PIMV) systems. Potential energy surfaces describing the main features of b) GSMV and c) PIMV systems.

Donor/Acceptor Inversion

In non-symmetric PIMV systems where C is not shuttled away from the MV core, its influence can be so strong that inverts the donor and acceptor roles with respect to the corresponding ground state analogs. We studied bimetallic $[Ru^{II}(tpy)(bpy)(\mu NC)M^{II/III}(CN)_5]^{n-}$, where M = Fe, Ru, Os, in water at room temperature (Figure 2).[34] Those complexes with M(III) ions are GSMV systems, with IVCT energies of 6700, 8800 and 9700 cm^{-1} for M = Ru(III), Os(III) and Fe(III), respectively. This trend follows the differences between the redox potentials of the {Ru(tpy)} and the $\{M(CN)_6\}$ moieties, of 0.33, 0.64 and 0.70 V, respectively. Therefore, the electronic configuration of the GSMV systems can be described as $\{Ru^{II+\delta}\text{-}M^{III-\delta}\}$, or {D–A}. From a molecular orbitals perspective, {Ru(tpy)} dπ orbitals lie below $\{M(CN)_6\}$ dπ orbitals. On the other hand, visible light photoexcitation of those complexes with M(II) afford {Ru(tpy)}-centered MLCT excited states. In this case, a PIMV system is formed where $tpy^{\bullet-}$ is the charge transfer counterpart C, which remains close to the PIMV core. Transient absorption spectroscopy with NIR detection permitted the observation of PIIVCT bands at 10000, 7800 and 7500 cm^{-1} for M = Ru(II), Os(II) and Fe(II), respectively. This trend is opposite to that of the redox potentials, and reveals a $\{(tpy^{\bullet-})Ru^{III-\delta}\text{-}M^{II+\delta}\}$ electronic configuration, or {(C)A–D}. The origin of this inversion in donor acceptor roles lies on electrostatic repulsion between $tpy^{\bullet-}$ and the dπ orbitals of the vicinal Ru ion. This repulsion is so strong that overcompensates the ground state redox asymmetry, and results in {Ru(tpy)} dπ orbitals lying above $\{M(CN)_6\}$ dπ orbitals. Key to this behavior is the non-symmetric nature of these PIMV systems. In the sections below, the reader will find discussions about the impact of C in symmetric PIMV systems. Those systems where C is distantly located from the PIMV core, essentially behave as their ground state {D–A} analogs,[25,33] although their photoinduced generation enables unique experimental conditions to study otherwise obscured scenarios.[26]

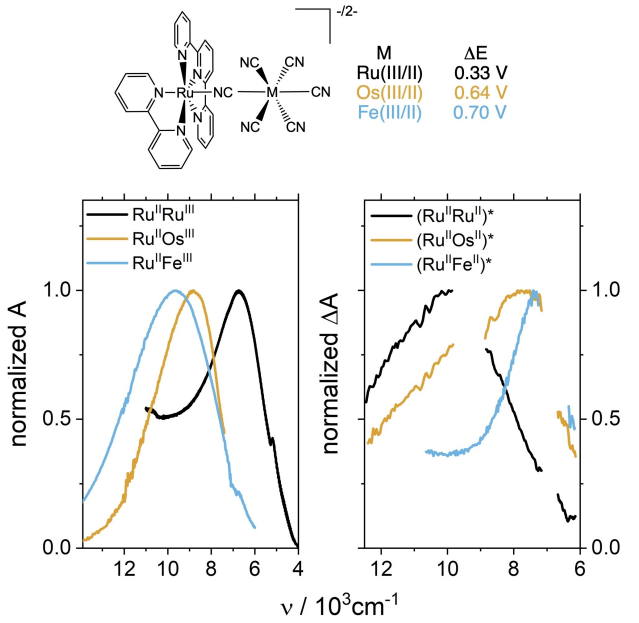

Figure 2. Top: Sketches of bimetallic $[Ru^{II}(tpy)(bpy)(\mu NC)M^{II/III}(CN)_5]^{-/2-}$. Bottom left: ground state IVCT absorptions (H_2O, room temperature). Bottom right: photoinduced IVCT absorptions obtained in TAS experiments (excitation at 505 nm, H_2O, room temperature). Adapted from Ref. [34] with permission from the Royal Society of Chemistry.

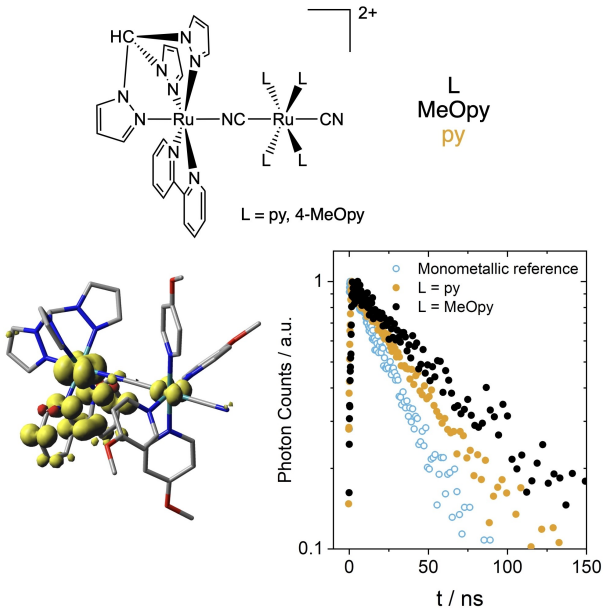

Figure 3. Top: Sketches of bimetallic $[Ru^{II}(tpm)(bpy)(\mu NC)Ru^{II}(L)_4(CN)]^{2+}$. Bottom left: DFT-calculated spin density of the lowest triplet state of the L = 4-MeOpy complex. Bottom right: TCSPC emission decays of the bimetallic complexes with L = py and 4-MeOpy, compared with that of the monometallic reference $[Ru^{II}(tpm)(bpy)(NCS)]^+$ (excitation at 505 nm, detection at 700 nm, DMSO, room temperature)

Hole Delocalization in MLCT Chromophores

In the bimetallic complexes described in the previous paragraph, PIIVCT absorption bands reveal orbital mixing in the MLCT excited state and some extent of hole delocalization. In comparison with $\{Ru^{III}(tpy^{\bullet-})\}$ MLCT states in monometallic references, in $\{(tpy^{\bullet-})Ru^{III-\delta}\text{-}M^{II+\delta}\}$ MLCT in bimetallic compounds the Ru(III) character of the MLCT-excited Ru(II) ion is attenuated to Ru(III-δ). Thanks to delocalization, $\{(tpy^{\bullet-})Ru^{III-\delta}\text{-}M^{II+\delta}\}$ is structurally more similar to the ground state than $\{Ru^{III}(tpy^{\bullet-})\}$, so its potential energy surface is more nested with that of the ground state. In consequence, non-radiative decay pathways are disfavored for the delocalized MLCT in bimetallic complexes, significantly prolonging their lifetimes. For example, TCSPC measurements yielded MLCT lifetimes of 5.4 ns of $[Ru^{II}(tpy)(bpy)(NCS)]^+$ in water, but 9.3 and 16.6 ns were obtained for $[Ru^{II}(tpy)(bpy)(\mu NC)M^{II}(CN)_5]^{2-}$ with M = Os and Ru, respectively.[34] A similar effect was observed for $[Ru^{II}(tpm)(bpy)(\mu NC)Ru^{II}(L)_4(CN)]^{2+}$, with L = pyridine (py) or 4-methoxypyridine (MeOpy). In this case, emission lifetimes of $\{(bpy^{\bullet-})Ru^{III-\delta}\text{-}M^{II+\delta}\}$ MLCT states, with PIIVCT bands at 8800 and 8100 cm^{-1}, were 49.4 and 51.5 ns for L = pyridine and 4-methoxypyridine, respectively in DMSO, *versus* only 30.5 ns for $[Ru^{II}(tpm)(bpy)(NCS)]^+$ (Figure 3).[35] Theoretical calculations support a delocalized electronic configuration for these complexes in their lowest triplet states. The DFT-calculated density of unpaired electrons for the optimized triplets is clearly distributed between both Ru ions, and Mulliken spin densities were 0.71 and 0.18 for both Ru ions when L = MeOpy, and 0.79 and 0.13 when L = py. TD-DFT affords computed electronic spectra that matched the experimental ones, including intense transitions of PIIVCT character calculated for both complexes at 8095 and 7263 cm^{-1}, respectively.

Coexistence of Excited States

Observation of PIIVCT bands can be exploited to resolve MLCT excited states of different wavefunction symmetries within a single chromophore and interpret their peculiar dynamics. In $[Ru^{II}(tpy)(bpy)(\mu CN)Ru^{II}(py)_4Cl]^{2+}$, visible light absorption populates the MLCT manifold.[36] Similar to other bimetallic complexes described above, intense NIR bands are observed in TAS, ascribed to PIIVCT transitions originating in a $\{(tpy^{\bullet-})Ru^{III-\delta}\text{-}M^{II+\delta}\}$ MLCT electronic configuration. However, decay of the ground state bleach, which indicates ground state recovery, was slower than the decay of the PIIVCT. This pointed to the participation of an additional excited state in the decay cascade. Target analysis of TAS data afforded differential spectra for two separate excited states (Figure 4). The first one, including an intense PIIVCT band, was ascribed to the $\{(tpy^{\bullet-})Ru^{III-\delta}\text{-}M^{II+\delta}\}$ MLCT state. The second one showed all the characteristics of a MLCT state, including a nanosecond lifetime, but displayed very weak NIR photoinduced absorptions and was very similar to the differential spectrum of the monometallic reference $[Ru^{II}(tpy)(bpy)(CN)]^+$. Therefore, its electronic configuration was assigned as a localized $\{(tpy^{\bullet-})Ru^{III}\text{-}M^{II}\}$ MLCT. This was, to the best of our knowledge, the first time that two MLCT excited states with different electronic configurations were demonstrated to coexist in the nanosecond timescale. Both states are

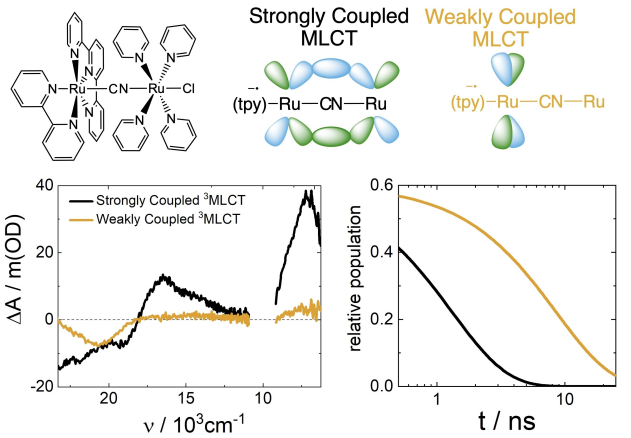

Figure 4. Top: Sketch of bimetallic $[Ru^{II}(tpy)(bpy)(\mu CN)Ru^{II}(py)_4Cl]^{2+}$, and schemes of coexisting MLCT states indicating the molecular orbital containing the excited hole. Bottom left: Differential spectra of the strongly coupled MLCT and the weakly coupled MLCT states obtained upon TAS (excitation at 387 nm, DMSO, room temperature). Bottom right: population evolution of the strongly coupled MLCT and the weakly coupled MLCT states over time.

described as {(C)A–D}, but they are PIMV systems of different Classes. On one hand, $\{(tpy^{\bullet-})Ru^{III-\delta}\text{-}M^{II+\delta}\}$ MLCT is a strongly coupled Class III or II/III system, with solvent independent PIIVCT energy and bandshape. DFT calculations on the lowest triplet afforded a completely delocalized configuration for the excited hole, in molecular orbitals parallel to the intermetallic axis, with Mulliken spin densities of 0.50 and 0.47 for both Ru ions. Crucially, the TD-DFT calculated PIIVCT band at 6925 cm^{-1} matches that one observed experimentally at 6900 cm^{-1}. On the other hand, $\{(tpy^{\bullet-})Ru^{III}\text{-}M^{II}\}$ MLCT is a weakly coupled Class I system, with no PIIVCT absorptions. In this excited state, the hole is completely localized in an orbital perpendicular to the intermetallic axis.[36] This Class I behavior is an excited state example of what has been observed in cyanide-bridged bimetallic compounds in the ground state, where electron donor ligands were placed in coordination positions perpendicular to the intermetallic axis, forcing hole localization.[37]

PIIVCT absorptions allowed not only to resolve the population of two MLCT states with different electronic configuration, but also enabled to monitor their reactivity in real time. Incorporation of a $\{Cr(CN)_6\}$ energy acceptor to the bimetallic Ru complex described in the previous paragraph yielded a trimetallic $[Ru^{II}(tpy)(bpy)(\mu CN)Ru^{II}(py)_4(\mu NC)Cr(CN)]$ complex, which showed Cr* emission after Ru-centered MLCT excitation, arising from an energy transfer process. However, a weak Ru-centered MLCT emission was still detectable, indicating that energy transfer was not complete. TAS revealed that the same two MLCT states as in the bimetallic model were populated. The intense PIIVCT band at 6900 cm^{-1} was observed to decay concomitantly with the rise of Cr* signals with a time constant of 106 ps, pointing to an efficient energy transfer process from the strongly coupled (Class III or II/III) MLCT to Cr*, where hole delocalization facilitated orbital overlap and a Dexter mechanism. In striking contrast, the perpendicular symmetry and localized nature of the weakly coupled (Class I) MLCT made it insensitive to the presence of the energy acceptor: no energy transfer takes place form this MLCT and its lifetime remains almost unchanged with respect to the bimetallic reference. This important discovery of bifurcated excited state reaction pathways was possible thanks to PIIVCT bands as wavefunction symmetry specific spectroscopic handles.[38]

Nature of Excited States in Earth-Abundant LMCT Chromophores

In high-valent iron chromophores, promising Earth-abundant scaffolds for sustainable energy conversion, LMCT states dominate light absorption, but short-lived metal-centered (MC) states play a crucial role in decay cascade.[39,40] In these complex systems, many different electronic configurations are accessible in the excited state decay cascade, and the observed dynamics are usually multiexponential. In this scenario, identification of spectroscopic handles that help to reveal the electronic structure of specific excited states and their dynamics is required. Thanks to PIIVCT bands, LMCT states and MC states can be successfully resolved in iron complexes with carbene-phenolate $\{(OCO^{2-})\}$ ligand scaffolds (Figure 5).[41] In $[Fe^{III}(OCO)_2]^-$, visible light excitation leads to $\{Fe^{II}(OCO^{2-})(OCO^-)\}$ LMCT states. They include a $\{(OCO^{2-})(OCO^-)\}$ ligand-based PIMV

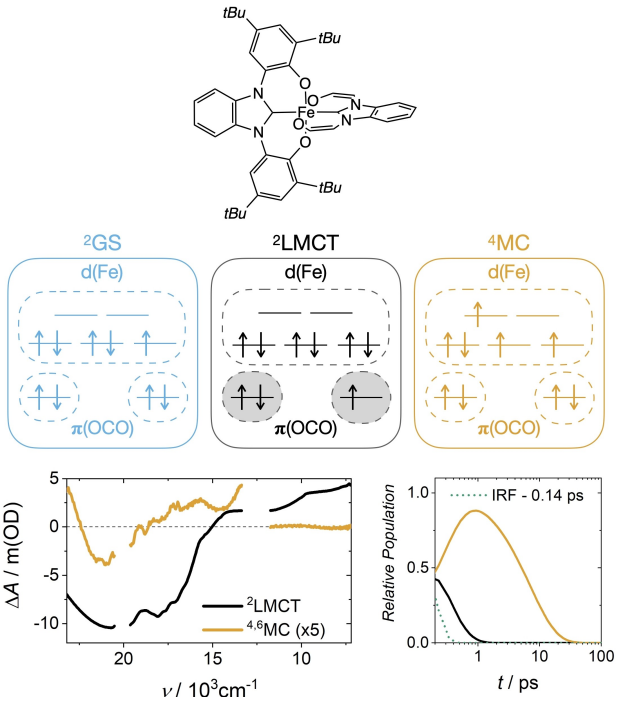

Figure 5. Top: Sketch of the $[Fe^{III}(OCO)_2]^-$ complex. Middle: Electronic structures of ^{2}GS, ^{2}LMCT and ^{4}MC states. The ligand-based PIMV system is highlighted in gray. Bottom left: Differential spectra of LMCT and MC states obtained upon TAS (excitation at 500 nm, toluene, room temperature). Bottom right: population evolution of LMCT and MC states over time.

core, and Fe(II) is both the charge transfer counterpart and the bridge connecting both ligands. Therefore, these LMCT states are {D-(C)-A} PIMV systems. Their differential spectra display optical activity in the NIR. In contrast, MC states are described with a $\{Fe^{III}*(OCO^{2-})(OCO^{2-})\}$ electronic configuration, lack any MV core and are NIR silent. In fact, target analysis of TA data for $[Fe^{III}(OCO)_2]^-$ indicated the participation of two excited states (Figure 5). First, the LMCT state, with a ground state bleach and an intense and broad PIIVCT in the NIR, that deactivates as fast as 200 fs. This process feeds a second excited state, MC, with a ground state bleach but NIR silent, that decays in 7 ps to the ground state.

Chemical oxidation of the Fe(III) complex affords a Fe(IV) chromophore, with slightly different excited state dynamics.[41] Excitation of $[Fe^{IV}(OCO)_2]$ leads to $\{Fe^{III}(OCO^{2-})(OCO^{-})\}$ LMCT states, with a ligand-based PIMV core and a Fe(III) counterpart and bridge. Thus, these states also are {D-(C)-A} PIMV systems, identical to the reduced complex in terms of D and A, but with C in a different oxidation state. This affords a PIIVCT energy shift from below 8000 cm^{-1} to 11000 cm^{-1} upon oxidation. Since both iron complexes are symmetric PIMV systems, the impact of C is equal for both D and A, and therefore its origins are related to an alteration of superexchange pathways that accompany the change in the electronic configuration of the Fe ion. For this of $[Fe^{IV}(OCO)_2]$ complex, LMCT states showing intense PIIVCT bands are observed in TAS. Their lifetime is only 11.8 ps, so they probably populate low lying MC states whose lifetime is too short to allow experimental detection.

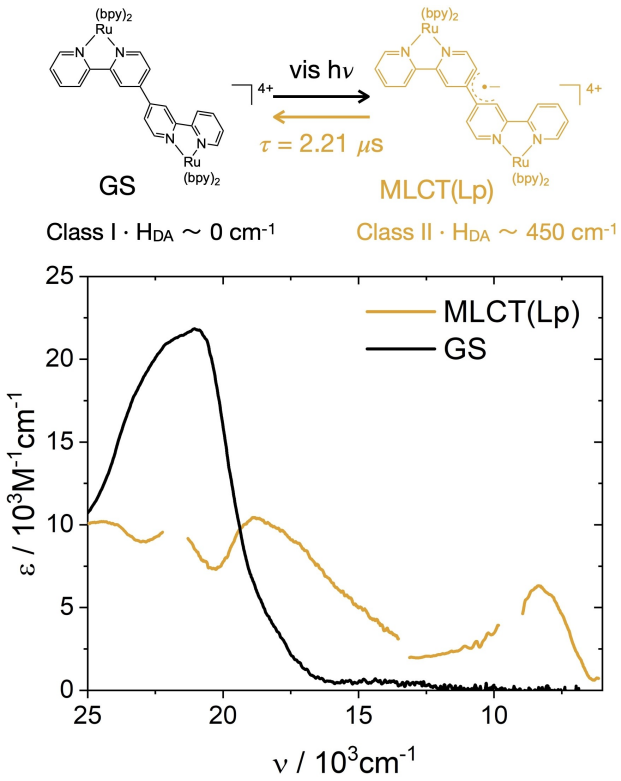

Figure 6. Top: Bimetallic $[Ru(bpy)_2(\mu Lp)Ru(bpy)_2]^{4+}$ approach a PIMV photoswitching behavior between a non-planar, Class I ground state and a planarized Class II MLCT state. Bottom: Absorption spectra of both species (ACN, room temperature). The absorption spectrum of the MLCT(Lp) state was reconstructed using TAS data (excitation at 460 nm), from where electronic coupling was derived. Adapted from Ref. [42] with permission from the PCCP Owner Societies.

Photoinduced Excited-State Isomerization Approaching a PIMV Molecular Photoswitch Behavior

PIMV systems allowed for developing a new concept in molecular electronics. Typically, molecular photoswitches are donor-acceptor systems where light absorption triggers reversible isomerization reactions. Electronic communication is strong in one of the isomers but negligible in the other, so light inputs can be used to turn electron transfer on and off. Recently, a very different strategy was proposed based on PIMV states (Figure 6).[42] $[Ru^{II}(bpy)_2(Lp)Ru^{II}(bpy)_2]^{4+}$, where Lp = 2,2′:4′,4″:2″,2‴-quaterpyridine, is a $\{Ru^{II}(bpy)_3\}$ dimer connected at the *para* positions of the bridging ligand. In the ground state, one electron electrochemical oxidation affords a $\{Ru^{II}(Lp)Ru^{III}\}$ core. This is a {D–A} MV system, which doesn't present any IVCT absorption and therefore it belongs to Class I, where both Ru ions are practically decoupled from each other. Nevertheless, photoexcitation with visible light populates the MLCT(Lp) state that, according to TAS, includes the fingerprint absorptions of the reduced Lp and significant PIIVCT absorptions at 8340 cm^{-1}. Therefore, its electronic configuration can be described as $\{Ru^{II+\delta}(Lp^{\bullet-})Ru^{III-\delta}\}$. This is a {D-(C)-A} Class II PIMV system, where the presence of C plays a determinant role. This MLCT state is a symmetric system, so the impact of C is related to changes in superexchange pathways upon bridge reduction. Lp is a biphenyl-type bridge, and can be interpreted as a chelating analogue of 4,4′-bipyridine. These ligands are known to undergo significant conformational changes upon reduction, in which the tilted biphenyl motif planarizes in a semiquinoid structure.[43] Planarization of the bridge enhances orbital overlap and boosts superexchange electronic coupling. Thus, despite virtually identical Ru–Ru distances, H_{DA} ~0 cm^{-1} in the tilted ground state, while H_{DA} >450 cm^{-1} in the planarized excited state. DFT calculations support this interpretation, with calculated dihedral angles of 30° for Lp in the ground state bimetallic complex, and 4° for $Lp^{\bullet-}$ in the MLCT state. The exceptional photostability[44] of $[Ru^{II}(bpy)_2(Lp)Ru^{II}(bpy)_2]^{4+}$ results in reversible on-off cycles corresponding to excitation-decay. However, the remaining challenge is to extend the stability of the high-energy species via lifetime extension, and to provide bidirectional control of the PIMV photoswitch.

Conclusions and Outlook

The detection and analysis of PIIVCT bands enabled the discovery of fundamental phenomena, like donor/acceptor inversion, coexistence of MLCT states of different symmetry up to the nanosecond timescale, and bifurcation of excited state

reaction pathways based on wavefunction symmetry. Additionally, PIIVCT bands are useful spectroscopic handles in Earth-abundant LMCT chromophores, that allow to determine the nature of the excited states that participate in the decay cascade. Furthermore, PIMV systems are the base of a new concept in the design of molecular photoswitches, that relies in conformational changes of bridging ligands upon optical/photoinduced charge transfers. With the availability of robust commercial TAS setups with NIR detection, the stage is set for PIIVCT bands to become a widespread tool in excited state electron transfer and in photochemistry.

Acknowledgements

The authors thank all colleagues and co-workers that participated in the research addressed in this review. A Cotic is a doctoral fellow of CONICET, and IRW is a doctoral fellow of UBA. AC is a member of the research staff of CONICET and a fellow of ALN. Funding from CONICET (PIP 11220200102757CO) and ANPCyT (PICT 2018-00924 and 2019-02410) is acknowledged. Open Access funding enabled and organized by Projekt DEAL.

Conflict of Interest

The authors declare no conflict of interest.

Keywords: photoinduced intervalence charge transfer · transient absorption spectroscopy · donor-acceptor interactions · excited-state dynamics · photoinduced mixed valence

[1] C. Creutz, H. Taube, *J. Am. Chem. Soc.* **1969**, *91*, 3988–3989.
[2] P. Day, N. S. Hush, R. J. H. Clark, *Philos. Trans. R. Soc. London* **2008**, *366*, 5–14.
[3] W. Kaim, G. K. Lahiri, *Angew. Chem. Int. Ed.* **2007**, *46*, 1778–1796; *Angew. Chem.* **2007**, *119*, 1808–1828.
[4] O. S. Wenger, *Chem. Soc. Rev.* **2012**, *41*, 3772–3779.
[5] M. D. Ward, *Chem. Soc. Rev.* **1995**, *24*, 121–134.
[6] J. C. Goeltz, B. J. Lear, C. P. Kubiak, *Eur. J. Inorg. Chem.* **2009**, 585–594.
[7] S. F. Nelsen, *Chem. A Eur. J.* **2000**, *6*, 581–588.
[8] K. D. Demadis, C. M. Hartshorn, T. J. Meyer, *Chem. Rev.* **2001**, *101*, 2655–2686.
[9] D. M. D'alessandro, F. R. Keene, *Chem. Soc. Rev.* **2006**, *35*, 424–440.
[10] J. Hankache, O. S. Wenger, *Chem. Rev.* **2011**, *111*, 5138–5178.
[11] L. Greb, *Eur. J. Inorg. Chem.* **2021**, DOI: 10.1002/ejic.202100871.
[12] W. E. Jones, P. Chen, T. J. Meyer, *J. Am. Chem. Soc.* **1992**, *114*, 387–388.
[13] R. Murase, C. F. Leong, D. M. D'Alessandro, *Inorg. Chem.* **2017**, *56*, 14373–14382.
[14] R. F. Winter, *Organometallics* **2014**, *33*, 4517–4536.
[15] B. S. Brunschwig, C. Creutz, N. Sutin, *Chem. Soc. Rev.* **2002**, *31*, 168–184.
[16] D. M. D'Alessandro, F. R. Keene, *Chem. Rev.* **2006**, *106*, 2270–2298.
[17] K. S. Schanze, T. J. Meyer, *Inorg. Chem.* **1985**, *24*, 2121–2123.
[18] K. S. Schanze, G. A. Neyhart, T. J. Meyer, *J. Phys. Chem.* **1986**, *90*, 2182–2193.
[19] Y. J. Chen, J. F. Endicott, V. Swayambunathan, *Chem. Phys.* **2006**, *326*, 79–96.
[20] J. F. Endicott, Y. J. Chen, *Inorg. Chim. Acta* **2007**, *360*, 913–922.
[21] J. V. Lockard, J. I. Zink, A. E. Konradsson, M. N. Weaver, S. F. Nelsen, *J. Am. Chem. Soc.* **2003**, *125*, 13471–13480.
[22] S. F. Nelsen, A. E. Konradsson, M. N. Weaver, I. A. Guzei, M. Goebel, R. Wortmann, J. V. Lockard, J. I. Zink, *J. Phys. Chem. A* **2005**, *109*, 10854–10861.
[23] J. V. Lockard, J. I. Zink, D. A. Trieber, A. E. Konradsson, M. N. Weaver, S. F. Nelsen, *J. Phys. Chem. A* **2005**, *109*, 1205–1215.
[24] W. Z. Alsindi, T. L. Easun, X. Z. Sun, K. L. Ronayne, M. Towrie, J. M. Herrera, M. W. George, M. D. Ward, *Inorg. Chem.* **2007**, *46*, 3696–3704.
[25] J. Petersson, J. Henderson, A. Brown, L. Hammarström, C. P. Kubiak, *J. Phys. Chem. C* **2015**, *119*, 4479–4487.
[26] R. N. Sampaio, E. J. Piechota, L. Troian-Gautier, A. B. Maurer, K. Hu, P. A. Schauer, A. D. Blair, C. P. Berlinguette, G. J. Meyer, *Proc. Nat. Acad. Sci.* **2018**, *115*, 7248–7253.
[27] K. Matsui, M. K. Nazeeruddin, R. Humphry-Baker, M. Grätzel, K. Kalyanasundaram, *J. Phys. Chem.* **1992**, *96*, 10587–10590.
[28] K. Kalyanasundaram, M. Grätzel, M. K. Nazeeruddin, *Inorg. Chem.* **1992**, *31*, 5243–5253.
[29] C. A. Bignozzi, R. Argazzi, C. Chiorboli, F. Scandola, R. B. Dyer, J. R. Schoonover, T. J. Meyer, *Inorg. Chem.* **1994**, *33*, 1652–1659.
[30] D. M. Dattelbaum, C. M. Hartshorn, T. J. Meyer, *J. Am. Chem. Soc.* **2002**, *124*, 4938–4939.
[31] C. N. Fleming, D. M. Dattelbaum, D. W. Thompson, A. Y. Ershov, T. J. Meyer, *J. Am. Chem. Soc.* **2007**, *129*, 9622–9630.
[32] C. Lambert, R. Wagener, J. H. Klein, G. Grelaud, M. Moos, A. Schmiedel, M. Holzapfel, T. Bruhn, *Chem. Commun.* **2014**, *50*, 11350–11353.
[33] J. Henderson, C. P. Kubiak, *Inorg. Chem.* **2014**, *53*, 11298–11306.
[34] B. M. Aramburu-Trošelj, P. S. Oviedo, I. Ramírez-Wierzbicki, L. M. Baraldo, A. Cadranel, *Chem. Commun.* **2019**, *55*, 7659–7662.
[35] B. M. Aramburu-Trošelj, P. S. Oviedo, G. E. Pieslinger, J. H. Hodak, L. M. Baraldo, D. M. Guldi, A. Cadranel, *Inorg. Chem.* **2019**, *58*, 10898–10904.
[36] P. S. Oviedo, G. E. Pieslinger, L. M. Baraldo, A. Cadranel, D. M. Guldi, *J. Phys. Chem. C* **2019**, *123*, 3285–3291.
[37] G. E. Pieslinger, B. M. Aramburu-Trošelj, A. Cadranel, L. M. Baraldo, *Inorg. Chem.* **2014**, *53*, 8221–8229.
[38] P. S. Oviedo, L. M. Baraldo, A. Cadranel, *Proc. Nat. Acad. Sci.* **2021**, *118*, e2018521118.
[39] J. K. McCusker, *Science* **2019**, *363*, 484–488.
[40] O. S. Wenger, *Chem. A Eur. J.* **2019**, *25*, 6043–6052.
[41] A. Cadranel, L. Gravogl, D. Munz, K. Meyer, *Chem. A Eur. J.* **2022**, DOI: 10.1002/chem.202200269.
[42] A. Cotic, S. Cerfontaine, L. Slep, B. Elias, L. Troian-Gautier, A. Cadranel, *Phys. Chem. Chem. Phys.* **2022**, DOI: 10.1039/D2CP01791A.
[43] C. C. Scarborough, S. Sproules, T. Weyhermüller, S. DeBeer, K. Wieghardt, *Inorg. Chem.* **2011**, *50*, 12446–12462.
[44] S. Cerfontaine, L. Troian-Gautier, S. A. M. Wehlin, F. Loiseau, E. Cauët, B. Elias, *Dalton Trans.* **2020**, *49*, 8096–8106.

Manuscript received: June 7, 2022
Revised manuscript received: July 1, 2022
Accepted manuscript online: July 4, 2022
Version of record online: August 3, 2022